Adaptive defect correction methods for viscous, incompressible flow problems

EINDHOVEN UNIVERSITY OF TECHNOLOGY
Department of Mathematics and Computing Science

RANA 98-30
December1998

Adaptive Defect Correction Methods for Viscous, Incompressible Flow Problems

by

V. Ervin, W. Layton, and J. Maubach

Reports on Applied and Numerical Analysis
Department of Mathematics and Computing Science
Eindhoven University of Technology
P.O. Box 513
5600 MB Eindhoven, The Netherlands
ISSN: 0926-4507

Adaptive Defect Correction Methods for Viscous, Incompressible Flow Problems

V. J. Ervin* W. J. Layton† J. M. Maubach

Institute for Computational Mathematics and Applications

Department of Mathematics and Statistics

University of Pittsburgh

Pittsburgh, PA 15260

email: ervinv@math.clemson.edu

wjl@vms.cis.pitt.edu

jmaubach@vms.cis.pitt.edu

Abstract

We consider a defect correction method which has been used extensively in applications where solutions have sharp transition regions, such as high Reynolds number fluid flow problems. A reliable a posteriori error estimator is derived for the defect correction method. The estimator is developed for two examples: a) the case of a linear-diffusion, nonlinear convection-reaction equation, and b) the nonlinear Navier-Stokes equations. Numerical experiments are provided which illustrate the utility of the resulting adaptive defect correction method for high Reynolds number, incompressible, viscous flow problems.

---

*On leave from the Department of Mathematical Sciences, Clemson University, Clemson S.C. 29634.

†Partially supported by NSF grant DMS-9400057.

1 Introduction

Defect correction methods were originally viewed as alternates to Richardson extrapolation for increasing the formal order of finite difference methods. Increasingly however, the development of the abstract theory for these procedures, see e.g., [5], [6], [10], [18], [30], [22], [23], [34], [38], as well as the computational practice of the methods, see e.g. [17], [24], [25], [26], [27], [28], have evolved to using defect correction to solve much harder, nearly singular, nonlinear problems through regularization and correction. This is somewhat surprising since solutions of representative applications such as high Reynolds number fluid flow problems [25], [26], [27], [28], [30], and convection-dominated, convection diffusion equations are characterized by sharp layers and transition regions. Thus, in spite of lacking the global smoothness required for the classical convergence analysis via asymptotic error expansions, global "uniform in epsilon" convergence in the smooth region has indeed been proven for defect correction methods in [5], [6], [18], and experimentally verified, [17], [24] - [28], even for these challenging applications.

For such problems, grid refinement in sharp transition regions is necessary in conjunction with the high accuracy attained in smooth regions by defect correction techniques. Reliability of the resulting self-adaptive, defect-correction procedure is then tied to the reliability of the a posteriori error estimator used for the defect correction discretization. We consider precisely this issue herein.

Section 2 provides an a posteriori error estimator for defect-correction methods for solving the general parameter dependent nonlinear problem $F(u\,,\,\epsilon) = 0$. The estimators are of the residual type for an abstract realization of the defect correction discretization. They are further developed and particularized for two representative applications: linear diffusion coupled with nonlinear convection (section 3) and (the targeted application) the incompressible Navier-Stokes equations (section 4).Section 5 gives some computational experiments with the resulting self-adaptive method.

To formulate the abstract problem, method and results, let X and Y be Banach spaces $A \in$

$\mathcal{L}(X, Y^*)$, $G(\cdot) \in C^1(X, Y^*)$ and $\epsilon \in \Lambda \subset \mathbb{R}$ Fréchet differentiable. The problem is now to solve

$$F(u, \epsilon) := A(\epsilon)u + G(u) = 0, \tag{1.1}$$

for $u = u(\epsilon)$. The abstract defect correction method is given as follows. Let $X_h, Y_h \subset X, Y$ (respectively) be finite dimensional subspaces and $A_h : X_h \to Y_h{}^*$, $G_h(\cdot) \in C^1(X_h, Y_h{}^*)$, be (finite dimensional) approximations of A and $G(\cdot)$ respectively.

Let $\epsilon_0 \geq \epsilon$, $A_h(\epsilon_0)$ a "stabilized" or regularized approximation to $A_h(\epsilon)$, and $J > 1$ be given. The method we are studying computes $u^1, \ldots, u^J \in X_h$ as follows. $u^1 \in X_h$ satisfies

$$F_h(u^1, \epsilon_0) := A_h(\epsilon_0)u^1 + G_h(u^1) = 0, \tag{1.2}$$

whereupon successive corrections are given by : *for* $j = 1, \ldots, J$,

$$A_h(\epsilon_0)u^{j+1} + G_h(u^{j+1}) = (A_h(\epsilon_0) - A_h(\epsilon))u^j . \tag{1.3}$$

There are numerous attractive practical features of (1.2), (1.3), cited in the above references. We take (1.2), (1.3) as the basic algorithm and work to find a computable upper bound for $||u - u^{j+1}||_X$. To realize 1.3, the iterand u^{j+1} is typically computed with a Newton method and is root of $\hat{F}_{\epsilon_0}(u) = 0$ with $\hat{F}_{\epsilon_0}(u) = A_h(\epsilon_0)u + G_h(u) + (A_h(\epsilon) - A_h(\epsilon_0))u^j$. If the regularization is performed carefully, we often observe that only one or two Newton steps suffice in order to solve (1.3) for u^{j+1}, beginning with u^j and that the resulting linearized systems are much cheaper to solve than are unregularized linear systems.

It is useful to think of (1.2) as an abstract realization of a convection-diffusion problem in which $A(\epsilon) \sim \epsilon A$. Suppose transition regions of the underlying physical problems are of width $\epsilon^{1/\alpha}$. Then, a typical choice for $A_h(\epsilon_0)$ involves increasing, on each mesh cell, ϵ to $\epsilon + O($ mesh cell diameter$^\alpha) \approx \epsilon + O(h^\alpha_{local})$. For example, $\epsilon + O(h)$ for convection diffusion problems and $\epsilon + O(h^2)$ for 2d incompressible, viscous flow problems.

Herein we take an approach related to the local residual error estimators of [4], [7], [8], [9], [16], [19], [43], as adapted to nonlinear problems in, for example, [43], [34]. In contrast to most of the work on

error estimators for parameterized nonlinear equations, in which the goal is to construct reliably and efficiently the solution manifold as a function of the system parameter, the goal of defect correction type methods is to solve a nearly singular , very large, nonlinear system (such as high Reynolds number fluid flow, [26]-[30]) via regularization by local effective viscosity adjustments followed via anti-diffusion by correction.

2 Preliminaries

The basic assumption on (1.1) under which we proceed is that u is a nonsingular solution of (1.1), i.e., $DF(u,\epsilon) = [A(\epsilon) + DG(u)] \in \text{Isom}(X, Y^*)$, and that $DG(\cdot)$ is Lipschitz continuous in some ball about the solution u.

Theorem 2.1 *Suppose that u is an isolated solution of (1.1) and that $DG(u)$ is Lipschitz continuous in some ball around u. Specifically, there is a $R_0 > 0$ such that*

$$\gamma := \sup_{w \in B(u;R_0)} \frac{||DG(w) - DG(u)||_{\mathcal{L}(X,Y^*)}}{||w - u||_X} < \infty .$$

Suppose that $u^j \in B(u;R)$ where

$$R := \min \left\{ R_0, \gamma^{-1} ||DF(u,\epsilon)^{-1}||^{-1}_{\mathcal{L}(Y^*,X)} \right\} . \tag{2.4}$$

Set $u^0 = 0$ and let u^j, $j = 1, \ldots, J$; be given by (1.2), (1.3). Let $R_h \in \mathcal{L}(Y, Y_h)$ be a restriction operator. Then $||u - u^{j+1}||_X$ is bounded as follows.

For $j = 1, \ldots, J-1$,

$$\begin{aligned} ||u - u^{j+1}||_X \leq 2||[A(\epsilon) &+ DG(u)]^{-1}||_{\mathcal{L}(Y^*,X)} \left\{ ||(I_Y - R_h)^* [A(\epsilon)u^{j+1} + G(u^{j+1})]||_{Y^*} \right. \\ &+ ||R_h||_{\mathcal{L}(Y,Y_h)} ||(A(\epsilon) - A_h(\epsilon))u^{j+1} + (G - G_h)(u^{j+1})||_{Y_h^*} \\ &+ \left. ||R_h||_{\mathcal{L}(Y,Y_h)} ||(A_h(\epsilon_0) - A_h(\epsilon))\,(u^{j+1} - u^j)||_{Y_h^*} \right\} . \end{aligned} \tag{2.5}$$

Proof : For R given by (2.4), and $w \in B(u,R) \subset X$,

$$w - u = DF(u,\epsilon)^{-1} \left\{ F(w,\epsilon) + \int_0^1 [DF(u,\epsilon) - DF(u + t(w-u),\epsilon)](w-u)\, dt \right.$$

$$- \; F(u,\epsilon) \quad \Big\}.$$

Therefore (as $F(u,\epsilon) = 0$),

$$\begin{aligned} ||w-u||_X \;&\leq\; ||DF(u,\epsilon)^{-1}||_{\mathcal{L}(Y^*,X)} \Big\{ \quad ||F(w,\epsilon) - F(u,\epsilon)||_{Y^*} \\ &\qquad + \int_0^1 ||DF(u,\epsilon) \;-\; DF(u+t(w-u),\epsilon)||_{\mathcal{L}(X,Y^*)} ||w-u||_X \, dt \Big\} \\ &\leq\; ||DF(u,\epsilon)^{-1}||_{\mathcal{L}(Y^*,X)} \, ||A(\epsilon)w \,+\, G(w)||_{Y^*} \\ &\qquad + \frac{1}{2} ||DF(u,\epsilon)^{-1}||_{\mathcal{L}(Y^*,X)} \;\gamma \, ||w-u||_X^2 \,. \end{aligned}$$

By assumption on R, $||DF(u,\epsilon)^{-1}||_{\mathcal{L}(Y^*,X)} \, \gamma \, ||w-u||_X \leq ||DF(u,\epsilon)^{-1}||_{\mathcal{L}(Y^*,X)} \gamma \cdot R \leq 1$. Thus,

$$||w-u||_X \leq ||DF(u,\epsilon)^{-1}||_{\mathcal{L}(Y^*,X)} ||A(\epsilon)w \,+\, G(w)||_{Y^*} \,+\, \frac{1}{2}||w-u||_X$$

and therefore,

$$\begin{aligned} ||w-u||_X \;&\leq\; 2||DF(u,\epsilon)^{-1}||_{\mathcal{L}(Y^*,X)} \; ||A(\epsilon)w \,+\, G(w)||_{Y^*} \\ &\leq\; 2||DF(u,\epsilon)^{-1}||_{\mathcal{L}(Y^*,X)} \; ||F(w,\epsilon)||_{Y^*} \,. \end{aligned}$$

The next step is to let $w := u^{j+1}$ and to use its determining equations (1.2), (1.3). To this end, consider

$$\begin{aligned} ||F(u^{j+1},\epsilon)||_{Y^*} \;&=\; \sup_{\phi \in Y} \frac{\left\langle A(\epsilon)u^{j+1} \,+\, G(u^{j+1}) \,,\, \phi \right\rangle}{||\phi||_Y} \\ &=\; \sup_{\phi \in Y} \Big\{ \left\langle A(\epsilon)u^{j+1} \,+\, G(u^{j+1}) \,,\, \phi \,-\, R_h\phi \right\rangle \\ &\qquad - \left\langle (A(\epsilon) - A_h(\epsilon))u^{j+1} \,+\, (G - G_h)(u^{j+1}) \,,\, R_h\phi \right\rangle \\ &\qquad + \left\langle (A_h(\epsilon_0) - A_h(\epsilon))(u^{j+1} - u^j) \,,\, R_h\phi \right\rangle \Big\} \,/||\phi||_Y \,. \end{aligned}$$

As, $R_h \in \mathcal{L}(Y, Y_h)$, it follows immediately that

$$\begin{aligned} ||F(u^{j+1},\epsilon)||_{Y^*} \;&\leq\; ||(I_Y - R_h)^* \, (A(\epsilon)u^{j+1} \,+\, G(u^{j+1}))||_{Y^*} \\ &\qquad + ||R_h||_{\mathcal{L}(Y,Y_h)} \, ||(A(\epsilon) - A_h(\epsilon))u^{j+1} \,+\, (G - G_h)(u^{j+1})||_{Y_h^*} \\ &\qquad + ||R_h||_{\mathcal{L}(Y,Y_h)} \, ||(A_h(\epsilon_0) - A_h(\epsilon))(u^{j+1} - u^j)||_{Y_h^*} \,, \end{aligned}$$

which completes the proof. ■

Remarks : The terms $A(\epsilon) - A_h(\epsilon)$, and $G - G_h$, represent consistency error terms and will normally be of higher order. Thus the error estimator will normally be dominated by the residual term $||(I_Y - R_h)^* (A(\epsilon)u^{j+1} + G(u^{j+1}))||_{Y^*}$ and the update $||(A_h(\epsilon_0) - A_h(\epsilon))(u^{j+1} - u^j)||_{Y_h^*}$. One example in which consistency error terms can be significant is when G_h includes terms arising from a subgridscale model added to the basic discretization.

3 A posteriori error estimators for a Linear Diffusion - Nonlinear Convection Problem

Let $\Omega \subset \mathbb{R}^2$, $X = Y := \overset{o}{W}{}^{2,1}(\Omega)$. Set $||u||_X = ||\nabla u||_{L^2(\Omega)}$ and define $F(u, \epsilon)$ via the Riesz representation theorem as the element of X^* satisfying

$$\langle F(u,\epsilon)\,,\,\phi\rangle \;:=\; \int_\Omega \left[\epsilon \nabla u \cdot \nabla \phi \,+\, g(\nabla u, u)\phi \,-\, f\phi\right] dx\,. \tag{3.6}$$

Then, u is a solution of $F(u, \epsilon) = 0$ in X if and only if u is a weak solution of the convection-diffusion-reaction equation :

$$\begin{cases} -\epsilon \triangle u \,+\, g(\nabla u, u) \,=\, f\,, \text{ in } \Omega \subset \mathbb{R}^2\,, \\ \qquad\qquad u \,=\, 0\,, \text{ on } \partial\Omega\,. \end{cases}$$

Let $X_h = Y_h \subset X$ be a conforming finite element space (assuming Ω is a polygonal domain), for specificity, suppose X_h contains C^0 piecewise polynomials of degree $\leq k$ on an edge-to edge triangulation of $\Pi^h(\Omega)$ of Ω. The triangulation, $\Pi^h(\Omega)$, is assumed to have its 'minimum angle' $\theta_{min}(\Pi^h(\Omega))$ bounded away from zero uniformly in h.

The usual Galerkin finite element approximation of (3.6) is given by : $F_h(w_h, \epsilon) = 0 \in X_h^*$ where, for all w_h, $\phi_h \in X_h$

$$\langle F_h(w_h,\epsilon)\,,\phi_h\rangle \;=\; \langle F(w_h,\epsilon)\,,\phi_h\rangle\;.$$

The operators A_h , $G_h(\cdot)$ are defined analogously to $F(\cdot,\cdot)$ via the Riesz representation theorem and the relations:

$$\langle A_h(\epsilon)w_h\,,\,\phi_h\rangle \;=\; \int_\Omega \epsilon\,\nabla w_h \cdot \nabla \phi_h\, dx\,,$$

$$\langle A_h(\epsilon_0)w_h\,,\,\phi_h\rangle \;=\; \sum_{T\in\Pi^h(\Omega)}\int_T (\epsilon + diam(T))\,\nabla w_h\cdot\nabla\phi_h\,dx\,,$$

$$\langle G_h(w_h)\,,\,\phi_h\rangle \;=\; \int_\Omega [g(\nabla w_h, w_h)\phi_h \;-\; f\phi_h]\,dx\,.$$

With these choices of F_h, A_h, and G_h, (1.2), (1.3) becomes the usual finite element, defect correction discretization of (3.6).

Provided, for example, $g(s,t)$ satisfies a growth condition and $\int_\Omega g(\nabla w, w)\,w\,dx \geq 0$ for $w \in X$, it can be shown that weak solutions of $F(u,\epsilon) = 0$ (3.6) exist. If $F(u,\epsilon)$ is monotone as a function of u, solutions are also unique (in the linear case, $g(\nabla w, w) \;=\; \mathbf{b}\cdot\nabla w \;+\; pw$, and this holds if $p \;-\; 1/2\,\nabla\cdot\mathbf{b} \geq 0$). We assume that, minimally, the solution u we approximate is non-singular in the sense that $D_u F(u,\epsilon)$ is invertible.

We also suppose that the finite element space admits the existence of an interpolation operator R_h of the Clément type. Specifically, $R_h\colon X \mapsto X_h$ satisfies the following elementwise error estimate (see [12]). For $\phi \in X$ there are $C_i = C_i(\theta_{min}(\Pi^h(\Omega)))$, $i = 1,2$, such that

$$\left.\begin{aligned} ||\phi \;-\; R_h\phi||_{W^{j-1,2}(T)} &\leq C_1 h_T^{2-j}||\phi||_{W^{1,2}(N(T))}\,, j = 1,2\,,\\ ||\phi \;-\; R_h\phi||_{L^2(e)} &\leq C_2 h_e^{1/2}||\phi||_{W^{1,2}(N(e))}\,, \end{aligned}\right\} \tag{3.7}$$

for all elements $T \in \Pi^h(\Omega)$ and all edges e of the elements. Here $N(T)$ and $N(e)$ denote the union of all the elements touching T and e respectively. Also h_e and h_T will denote, as usual, the diameters of an edge e respectively element T.

For the first term on the right hand side of (2.5) we have, for $\phi \in Y$, $||\phi||_Y = 1$,

$$\left\langle (I_Y - R_h)^*\,[A(\epsilon)u^{j+1} \;+\; G(u^{j+1})]\,,\phi\right\rangle = \left\langle A(\epsilon)u^{j+1} \;+\; G(u^{j+1})\,,\phi \;-\; R_h\phi\right\rangle$$

$$= \sum_{T\in\Pi^h(\Omega)}\int_T \epsilon\nabla u^{j+1}\cdot\nabla(\phi - R_h\phi) + [g(\nabla u^{j+1}\,,u^{j+1}) - f](\phi - R_h\phi)\,dx\,.$$

Integration by parts over each $T \in \Pi^h(\Omega)$ and denoting the collection of interior edges in $\Pi^h(\Omega)$ by $E^h(\Omega)$, with the use of estimates like

$$\sum_T ||r^{j+1}||_{L^2(T)}||\phi||_{W^{1,2}(N(T))} \;\leq\; \left(\sum_T ||r^{j+1}||_{L^2(T)}\right)||\phi||_{W^{1,2}(\Omega)}$$

$$\leq \; C\sqrt{\sum_{T} ||r^{j+1}||^2_{L^2(T)}}\,||\phi||_{W^{1,2}(\Omega)},$$

yields

$$\begin{aligned}
&\left\langle (I_Y - R_h)^* \left[A(\epsilon)u^{j+1} + G(u^{j+1})\right],\, \phi \right\rangle \\
= \;& \sum_{T\in\Pi^h(\Omega)} \int_T \left(-\epsilon\triangle u^{j+1} + g(\nabla u^{j+1}, u^{j+1}) - f\right)(\phi - R_h\phi)\, dx \\
&+ \sum_{e\in E^h(\Omega)} \int_e \epsilon(\nabla u^{j+1}\cdot \mathbf{n}_e)\,(\phi - R_h\phi)\, de \\
\leq \; & C_1 \sum_{T\in\Pi^h(\Omega)} ||r^{j+1}||_{L^2(T)}\, h_T\, ||\phi||_{W^{1,2}(N(T))} \\
&+ C_2\,\epsilon \sum_{e\in E^h(\Omega)} ||[\nabla u^{j+1}\cdot \mathbf{n}_e]_e||_{L^2(e)}\, h_e^{1/2}\, ||\phi||_{W^{1,2}(N(e))} \\
\leq \; & C\left[\sum_{T\in\Pi^h(\Omega)} h_T^2\, ||r^{j+1}||^2_{L^2(T)} + \epsilon^2 \sum_{e\in E^h(\Omega)} h_e\, ||[\nabla u^{j+1}\cdot \mathbf{n}_e]_e||^2_{L^2(e)}\right]^{1/2} ||\phi||_{W^{1,2}(\Omega)},
\end{aligned}$$

where r^{j+1} is the residual, defined per mesh element T by $r^{j+1} := f - (-\epsilon\triangle u^{j+1} + g(\nabla u^{j+1}, u^{j+1}))$, $C = C(C_1, C_2, \theta_{min}(\Pi^h(\Omega)))$ is a computable constant, and $[u]_e$ denotes the jump of u across edge e.

With the usual conforming finite element formulation specified in this example, the second term in the right hand side of (2.5) is identically zero. To see this note that for all $\phi_h \in Y_h$, $\left\langle F(u^{j+1},\epsilon)\,,\, \phi_h\right\rangle = \left\langle F_h(u^{j+1},\epsilon)\,,\, \phi_h\right\rangle$, so that

$$\begin{aligned}
&||(A(\epsilon) - A_h(\epsilon))u^{j+1} + (G - G_h)(u^{j+1})||_{Y_h^*} \\
= \;& \sup_{\phi_h\in Y_h} \left\langle (A(\epsilon) - A_h(\epsilon))u^{j+1} + (G - G_h)(u^{j+1})\,,\, \phi_h\right\rangle \\
= \;& \sup_{\phi_h\in Y_h} \left\langle F(u^{j+1},\epsilon) - F_h(u^{j+1},\epsilon)\,,\, \phi_h\right\rangle = 0\,.
\end{aligned}$$

As for the last term, let $\phi_h \in Y_h$, $||\phi_h||_Y = 1$. Then,

$$\left\langle (A_h(\epsilon_0) - A_h(\epsilon))\,(u^{j+1} - u^j)\,, \phi_h\right\rangle \;=\; \int_\Omega (\epsilon_0 - \epsilon)\,\nabla(u^{j+1} - u^j)\cdot\nabla\phi_h\, dx$$

$$\leq \left[\sum_{T \in \Pi^h(\Omega)} ||(\epsilon_0 - \epsilon)\, \nabla(u^{j+1} - u^j)||^2_{L^2(T)} \right]^{1/2} .$$

Combining these terms gives the following error estimate for the method (1.2), (1.3):

$$\begin{aligned} ||u - u^{j+1}||_{W^{1,2}(\Omega)} \;\leq\; & C\, ||DF(u,\epsilon)^{-1}||_{\mathcal{L}(Y^*,X)} \left\{ \sum_{T \in \Pi^h(\Omega)} h_T^2\, ||r^{j+1}||^2_{L^2(T)} \right. \\ & + \epsilon^2 \sum_{e \in E^h(\Omega)} h_e\, ||[\nabla u^{j+1} \cdot \mathbf{n}_e]_e||^2_{L^2(e)} \\ & \left. + \sum_{T \in \Pi^h(\Omega)} ||\,(\epsilon_0 - \epsilon)\, \nabla(u^{j+1} - u^j)\,||^2_{L^2(T)} \right\}^{1/2} . \end{aligned} \tag{3.8}$$

In order to ensure full reliability, it remains to estimate $||DF(u,\epsilon)^{-1}||_{\mathcal{L}(Y^*,X)}$. This depends of course upon the precise nonlinearity $g(\nabla u, u)$. In general, $||DF(u,\epsilon)^{-1}||_{\mathcal{L}(Y^*,X)}$ can be approximated by $||DF(u^{j+1},\epsilon)^{-1}||_{\mathcal{L}(Y_h^*,X_h)}$ (this involves the solution of an eigenvalue problem). In some cases this multiplier can be bounded analytically. To illustrate this, let us assume that $g(\nabla w, w) = f + \underline{b}\cdot\nabla w + pw$ where $p - \nabla\cdot\underline{b}/2 \geq p_0 > 0$. Under this assumption a solution ϕ to $A(\epsilon)\phi + G(\phi) = 0$ exists for any $f \in Y^*$. Straightforward manipulations immediately give

$$\epsilon||\nabla\phi||_{L^2(\Omega)} \leq C||f||_{W^{-1,2}(\Omega)}$$

so that, in this case of a linear problem,

$$||DF(u,\epsilon)^{-1}||_{\mathcal{L}(Y^*,X)} \leq C\epsilon^{-1} .$$

However, in the most interesting cases this common multiplier must be approximated (as noted above), or estimated in an ad-hoc way via data-fitting.

4 Application to the Navier-Stokes Equations

Let $d = 2, 3$ be the dimension of the polygonal domain Ω, and let L^2_0 be the space of Lebesgue square integrable functions with zero mean average. Define $X = Y := ((\overset{o}{W}{}^{1,2}(\Omega))^d, L^2_0(\Omega))$ with norm of $\tilde{\mathbf{u}} = (\mathbf{u}, p) \in X$ given by

$$||\tilde{\mathbf{u}}||_X := [||\nabla\mathbf{u}||^2_{L^2(\Omega)} + ||p||^2_{L^2(\Omega)}]^{1/2} .$$

Define, via the Riesz representation theorem $F(\tilde{\mathbf{u}}, \epsilon)$ as that element of X^* satisfying

$$< F(\tilde{\mathbf{u}}, \epsilon), \tilde{\mathbf{v}} > = \int_\Omega [\epsilon \nabla \mathbf{u} : \nabla \mathbf{v} \ + \mathbf{u} \cdot \nabla \mathbf{u} \cdot \mathbf{v} \ + \ q(\nabla \cdot \mathbf{u} - g) \ - \ p \nabla \cdot \mathbf{v} - \mathbf{f} \cdot \mathbf{v}] \, dx \, , \text{ for all } \tilde{\mathbf{v}} \in X \, ,$$

where $\epsilon = \mathrm{Re}^{-1}$ is the inverse of the Reynolds number, $\tilde{\mathbf{u}} = (\mathbf{u}, p) \in X$ and $\tilde{\mathbf{v}} = (\mathbf{v}, q) \in X$.

The problem of solving $F(\tilde{\mathbf{u}}, \epsilon) = 0$ for $\tilde{\mathbf{u}} \in X$ is the equivalent to that of finding the weak solution $\tilde{\mathbf{u}} = (\mathbf{u}, p) \in X$ to the Navier-Stokes equations with $\epsilon = \mathrm{Re}^{-1}$:

$$\left.\begin{aligned} -\mathrm{Re}^{-1} \triangle \mathbf{u} + \mathbf{u} \cdot \nabla \mathbf{u} + \nabla p = \mathbf{f} \text{ in } \Omega, \ \mathbf{u} = \mathbf{0} \text{ on } \partial\Omega \\ \nabla \cdot \mathbf{u} = g \text{ in } \Omega \, , \ \textstyle\int_\Omega p \, dx = 0 \, . \end{aligned}\right\} \tag{4.9}$$

Given an edge to edge triangulation of Ω, $\Pi^h(\Omega)$, whose minimum angle θ_{min} is bounded away from zero, velocity-pressure finite element spaces can then be constructed on $\Pi^h(\Omega)$. We assume each possess an interpolation operator of the Clément type (satisfying 3.7). See [12] and [20] for examples.

Let (V^h, Q^h) denote those velocity-pressure finite element spaces which are assumed additionally to satisfy the inf-sup (or Babuska-Brezzi) condition [20], [21]. Specifically, there is a $\beta > 0$, independent of h, such that

$$\inf_{0 \neq q \in Q^h} \sup_{0 \neq \mathbf{v} \in V^h} \frac{\int_\Omega q \, \nabla \cdot \mathbf{v} \, dx}{\|\nabla \mathbf{v}\|_{L^2(\Omega)} \, \|q\|_{L^2(\Omega)}} \geq \beta > 0 \, . \tag{4.10}$$

The usual Galerkin-finite element approximation to (4.9) is then given by : $F_h(\tilde{\mathbf{u}}^h, \epsilon) = 0$ where, for all $\tilde{\mathbf{w}}_h, \tilde{\phi}_h \in X^h := (V^h, Q^h)$, $F_h(\cdot, \cdot)$ is defined by

$$< F_h(\tilde{\mathbf{w}}_h, \epsilon), \tilde{\phi}_h > := < F(\tilde{\mathbf{w}}_h, \epsilon), \tilde{\phi}_h > \ .$$

A_h and G_h are defined analogously to section 3 by

$$< A_h(\epsilon) \tilde{\mathbf{w}}_h, \tilde{\phi}_h > := \sum_{T \in \Pi^h(\Omega)} \int_T \epsilon \, \nabla \mathbf{w}_h : \nabla \phi_h \, dx \, ,$$

$$< G_h(\tilde{\mathbf{w}}_h), \tilde{\phi}_h > := < F_h(\tilde{\mathbf{w}}_h, \epsilon) \ - \ A_h(\epsilon) \tilde{\mathbf{w}}_h, \tilde{\phi}_h > \, ,$$

where $\tilde{\mathbf{w}}_h = (\mathbf{w}_h, q) \in X^h$, $\tilde{\phi}_h := (\phi_h, \lambda) \in X^h$.

With these choices of A_h, ϵ, $\epsilon_0(T) := max\{\epsilon, diam(T)\}$ and $G_h(\cdot)$, (1.2), (1.3) reduces to the usual finite element, nonlinear defect correction discretization of the incompressible Navier-Stokes equations (see e.g. [20], [21]). It is often highly advantageous in the algorithhm to perturb $G_h(\cdot)$ through

local averaging or the use of "flux limiters", see [26], [27], [28], or through the incorporation of an appropriate subgridscale model. For example, the incorporation of the model suggested in [31] (which we use herein) is equivalent to defining $G_h(\cdot)$ as :

$$< G_h(\tilde{\mathbf{w}}_h), \tilde{\phi}_h >:=< F_h(\tilde{\mathbf{w}}_h, \epsilon) - A_h(\epsilon)\tilde{\mathbf{w}}_h \, , \, \tilde{\phi}_h > + < \mu(h, Re) \, |\nabla \mathbf{w}_h|^r \nabla \mathbf{w}_h \, , \, \nabla \phi_h > ,$$

where the scaling term $\mu(h, Re)$ and exponent r are discussed in [31]. This incorporation adds one additional term to the right hand side of the error estimator but does not otherwise appreciably alter the following analysis. Letting $\tilde{\phi} \in Y$, $\|\tilde{\phi}\|_Y = 1$ be given and consider the first term on the right hand side of (2.5) :

$$< (I_Y - \tilde{R}_h)^*[A(\epsilon)\tilde{\mathbf{u}}^{j+1} + G(\tilde{\mathbf{u}}^{j+1})] \, , \, \tilde{\phi} > = < A(\epsilon)\tilde{\mathbf{u}}^{j+1} + G(\tilde{\mathbf{u}}^{j+1}) \, , \, \tilde{\phi} - \tilde{R}_h\tilde{\phi} >$$

$$= \sum_{T \in \Pi^h(\Omega)} \int_T [\, \epsilon \nabla \mathbf{u}^{j+1} : \nabla(\phi - R_h^V \phi) + \mathbf{u}^{j+1} \cdot \nabla \mathbf{u}^{j+1} \cdot (\phi - R_h^V \phi) + (q - R_h^Q q) \nabla \cdot \mathbf{u}^{j+1}$$
$$- \; p^{j+1} \nabla \cdot (\phi - R_h^V \phi) - g \cdot (q - R_h^Q q) - \mathbf{f} \cdot (\phi - R_h^V \phi) \,] \, dx$$

where $\tilde{\phi} = (\phi, q)$. Integration by parts over each $T \in \Pi^h(\Omega)$ and, denoting the collection of faces (3-D), or edges (2-D), of $\Pi^h(\Omega)$ in the interior of Ω by $E^h(\Omega)$, gives :

$$< (I_Y - \tilde{R}_h)^*[A(\epsilon)\tilde{\mathbf{u}}^{j+1} + G(\tilde{\mathbf{u}}^{j+1})] \, , \, \tilde{\phi} > =$$
$$\sum_{T \in \Pi^h(\Omega)} \int_T -\mathbf{r}^{j+1} \cdot (\phi - R_h^V \phi) + \int_T (q - R_h^Q q)(\nabla \cdot \mathbf{u}^{j+1} - g) \, dx$$
$$+ \sum_{e \in E^h(\Omega)} \int_e \epsilon \, [\nabla \mathbf{u}^{j+1} \cdot \mathbf{n}_e]_e \cdot (\phi - R_h^V \phi) - [p]_e \, (\phi - R_h^V \phi) \cdot \mathbf{n}_e \, d\sigma \, ,$$

where $\mathbf{r}^{j+1} := \mathbf{f} - (-\mathrm{Re}^{-1} \triangle \mathbf{u}^{j+1} + \mathbf{u}^{j+1} \cdot \nabla \mathbf{u}^{j+1} + \nabla p^{j+1})$.

Using the Cauchy -Schwartz inequality on each element T, and face (or edge) e, and the properties of $\tilde{R}_h\tilde{\phi}$ from (3.7) gives :

$$< (I_Y - \tilde{R}_h)^*[A(\epsilon)\tilde{\mathbf{u}}^{j+1} + G(\tilde{\mathbf{u}}^{j+1})] \, , \, \tilde{\phi} > \leq$$
$$C \left[\sum_{T \in \Pi^h(\Omega)} h_T^2 \|\mathbf{r}^{j+1}\|_{0,T}^2 + \|\nabla \cdot \mathbf{u}^{j+1} - g\|_{0,\Omega}^2 \right]^{1/2}$$
$$+ \; C \left[\sum_{e \in E^h(\Omega)} h_e \, \|[\mathrm{Re}^{-1} \nabla \mathbf{u}^{j+1} \cdot \mathbf{n}_e - p^{j+1} \mathbf{n}_e]_e\|_{0,e}^2 \right]^{1/2} ,$$

which is a bound on the first term on the right hand side of (2.5).

If the usual Galerkin formulation is used (i.e., no "subgridscale" modelling, numerical integration or other variational crime) then, as in the previous example, the second term on the right hand side of (2.5) is identically zero. As for the last term which involves $A_h(\epsilon_0) - A_h(\epsilon)$, let $\tilde{\phi} \in Y$ satisfy $\|\tilde{\phi}\|_Y = 1$. Then,

$$\begin{aligned} < (A_h(\epsilon_0) - A_h(\epsilon))(\tilde{\mathbf{u}}^{j+1} - \tilde{\mathbf{u}}^j), \tilde{\phi} > &= \int_\Omega (\epsilon_0 - \epsilon) \nabla(\mathbf{u}^{j+1} - \mathbf{u}^j) : \nabla\phi \, dx \\ &\leq \left[\sum_{T \in \Pi^h(\Omega)} \|(\epsilon_0(T) - \epsilon) \nabla(\mathbf{u}^{j+1} - \mathbf{u}^j)\|^2_{0,T} \right]^{1/2}. \end{aligned}$$

Combining these terms gives an error estimator :

$$\|\mathbf{u} - \mathbf{u}^{j+1}\|_1 + \|p - p^{j+1}\| \tag{4.11}$$

$$\begin{aligned} \leq\ & C \|DF(\tilde{\mathbf{u}}, \epsilon)^{-1}\|_{\mathcal{L}(Y^*, X)} \left\{ \left[\sum_{T \in \Pi^h(\Omega)} h_T^2 \|\mathbf{r}^{j+1}\|^2_{0,T} + \|\nabla \cdot \mathbf{u}^{j+1} - g\|^2_{0,T} \right]^{1/2} \right. \\ & + \left[\sum_{e \in E^h(\Omega)} h_e \|[\mathrm{Re}^{-1} \nabla \mathbf{u}^{j+1} \cdot \mathbf{n}_e - p^{j+1} \mathbf{n}_e]_e\|^2_{0,e} \right]^{1/2} \\ & \left. + \left[\sum_{T \in \Pi^h(\Omega)} \|(\epsilon_0(T) - \epsilon) \nabla(\mathbf{u}^{j+1} - \mathbf{u}^j)\|^2_{0,T} \right]^{1/2} \right\}. \end{aligned} \tag{4.12}$$

Remark: If the aforementioned subgridscale model from [31] is used in the residual calculator, then an extra term appears on the right hand side of this estimate. This term takes the form

$$\left[\sum_{T \in \Pi^h(\Omega)} \|\mu(h_T, Re) |\nabla \mathbf{u}^j|^r \nabla \mathbf{u}^j\|^2_{L^2(T)} \right]^{1/2}.$$

It remains, of course, to evaluate $\|DF(\tilde{\mathbf{u}}, \epsilon)^{-1}\|_{\mathcal{L}(Y^*, X)}$. The Navier-Stokes equations are not monotone so an a priori bound of this term for all possible solutions is not possible. (Singular solutions do exist and correspond to physically interesting flow situations.) Since $\|DF(\tilde{\mathbf{u}}, \epsilon)^{-1}\|_{\mathcal{L}(Y^*, X)}$ is a common multiplier of the right hand side of (4.12), it is not required for mesh redistribution, only for the computation of a reliable upperbound in order to check if a final stopping criterion is satisfied. Unfortunately, in general, this multiplier can only be estimated by, for example, solving an eigenvalue problem on a course mesh. This amounts to replacing $\|DF(\tilde{\mathbf{u}}, \epsilon)^{-1}\|_{\mathcal{L}(Y^*, X)}$ by $\|DF(\tilde{\mathbf{u}}^{j+1}, \epsilon)^{-1}\|_{\mathcal{L}(X^{H*}, X^H)}$ where $H >> h$.

5 Numerical Results

We give an illustration of the effectiveness of using defect correction methods, with a subgridscale (SGS) model, in an adaptive calculation. To illustrate the method we solve an equilibrium, high Reynolds number flow problem (4.9) via the Defect Correction Method (DCM) presented in section 1. In the tests presented herein, we either use the $k = 1$ accurate mini-element, Arnold, Brezzi and Fortin [1], or the second order accurate Taylor-Hood pair, Taylor and Hood [40].

The nonlinear systems arising at each step of the method, denoted $F(x) = 0$ were linearized by a Damped Inexact Newton Method [14], with stopping criterion $||F(x)||_2 < 10^{-8}$. The resulting non-symmetric linearized systems were solved with Sonneveld's Conjugate Gradient Squared (CGS) in [37] (with a Vanka-like ILU(0) preconditioner [42]). The Generalized Minimal Residual method (GMRES) of Saad and Schultz in [36], or Axelsson's Generalized Conjugate Gradient Least Squares method (GCGLS) in [2], [3] can also be used. However, it is our experience that they can consume more computational time because they explicitly orthogonalize search directions. The storage of all or several search directions further limits the amount of degrees of freedom which can be handled. The pressure was normalized by fixing its value in one point of the domain.

The initial guess for calculations on each newly refined grid is the solution interpolated from the previous grid. Grid to grid interpolation is easy because the grid refinement employed (see [32]) is hierarchical with conforming basis functions. Thus, the hierarchical mesh levels automatically provide accurate initial guesses to the non-linear solver. The few non-linear iterations (Newton steps) required reflects both this good initial guess and the regularization of the system inherent in DCM.

We have purposely used the most conservative options at each step because we are testing the viability of the basic defect correction method, rather than the many possible efficiency improvements. For example, the linear and non-linear systems were solved to essentially machine precision (rather than truncation error of the step in question). For the same reason, on each new mesh, DCM is restarted with an artificial viscosity solve followed by the corrections.

For every grid, first the artificial diffused system (1.2) is solved, with $\epsilon_0 = \epsilon + h^\alpha$. Next, k – the polynomial degree of the velocity approximation – anti-diffusive defect correction steps (1.3) follow, one step for the mini-element (although the extra added basis function is a polynomial of degree three) and two steps for the Taylor-Hood pair.

The stopping criterion used was the standard residual-based one $||r^{(l)}||_2 < 10^{-11}$, where $r^{(l)}$ is the l-th *updated residual*. In all examples, the nodes were numbered left to right and bottom to up. As usual, the ILU(0) preconditioner performs best for lower degree polynomial velocity approximations, when mesh refinement is limited, and when nodal support points are numbered regularly. In spite of this, we experienced no difficulties using a simple ILU(0) preconditioner, because the systems we solve arise from a regularized artificial viscosity approximation.

The coefficients of the discrete systems were computed with quadrature rules of degree $2k$. All quadrature rules employed use quadrature points strictly inside the reference element. In the case of $k = 1$, for instance, we used rule "T_2: 5-1" of degree 5 from Stroud [39], page 314. For higher polynomial degree k, quadrature formulas were taken from Dunavant [15]. The jump integrals over the edges, were computed with a standard Gauss-Legendre formula which is exact for all polynomials of degree $2k$.

All numerical experiments use the same mesh refinement technique. The coarse grids are of the Tucker-Whitney triangular type described by Todd [41]. The grid refinement by Maubach [32] and [33] was used to create the finer uniform and adaptively locally refined meshes.

The local error indicators are based on the estimator (4.12). For an element T, we measure the local error indicator, including a possible SGS model,

$$\begin{aligned} Est_\alpha^2(T) &= C_1^2 \left[h_T^2 ||\mathbf{r}^{j+1}||_{0,T}^2 + ||\nabla \cdot \mathbf{u}^{j+1} - g||_{0,T}^2 \right] \\ &+ C_2^2 \left[\sum_{e \in T} h_e \, ||[\mathrm{Re}^{-1} \nabla \mathbf{u}^{j+1} \cdot \mathbf{n}_e - p^{j+1} \mathbf{n}_e]_e||_{0,e}^2 \right] \\ &+ C_3^2 \left[||(\epsilon_0(T) - \epsilon) \nabla (\mathbf{u}^{j+1} - \mathbf{u}^j) + \mu(h_T, Re) |\nabla \mathbf{u}^j|^r \nabla \mathbf{u}^j||_{0,T}^2 \right] . \end{aligned} \tag{5.13}$$

The local error indicators sum up to our global error estimate

$$Est_\alpha^2(\Omega) := \sum_{T\in\Pi^h(\Omega)} Est_\alpha^2(T) \tag{5.14}$$

The estimated error for T, $Est_\alpha(T)$, depends on the amount of artificial viscosity $\epsilon_0 - \epsilon =: h^\alpha$. Here we choose $\alpha > 0$, a real number, and $h = h_T$, the diameter of triangle T. The usual choice for convection dominated convection diffusion problems (see [5], [18], [24] and [30]) is $\alpha = 1$. Since these problems typically have $O(\epsilon)$ outflow type layers, first, we test this usual choice for convection diffusion problems for the equilibrium Navier-Stokes equations.

The effect of the amount of artificial diffusion $h^\alpha = \epsilon_0 - \epsilon$ for DCM is explored, with the use of an example borrowed from Kwon, Layton and Peterson [29].

Test Problem 5.1 With the domain $[0,1]^2$, we take an exact solution $(\mathbf{u}, p)$ given below and, by substitution, obtain a right hand size $f = f(x, y, Re)$:

$$\mathbf{u}_1 = \sin\pi x \sin 2\pi x; \quad \mathbf{u}_2 = x^2(1-x)\sin\pi y; \quad p = (1 + y(y^2-4))\cos\pi x.$$

The velocity $\mathbf{u}$ satisfied the homogeneous Dirichlet boundary conditions. Note that the true solution is smooth uniformly in the Reynolds number.

We take $Re = 10^4$, set $C_1 = C_2 = C_3 = 1$, and compute $Est_\alpha^2(\Omega)$ and the true error in the energy norm for the discretization using a Taylor-Hood finite element approximation (conforming piecewise quadratic velocities and piecewise linear pressure) In our tests, achieving a preassigned stopping criterion is not primary. Rather then estimating the common multiplier $||DF^{-1}||$, we tabulate the ratios of the estimated errors $Est_\alpha(\Omega)/Est_1(\Omega)$ and the true errors $Err_\alpha(\Omega)/Err_1(\Omega)$. The energy norm errors are defined, as usual, by

$$Err_\alpha^2(\Omega) := \sum_{T\in\Pi^h(\Omega)} Err_\alpha^2(T), \quad Err_\alpha^2(T) := |\mathbf{u} - \mathbf{u}^{j+1}|_{1,T}^2 + ||p - p^{j+1}||_{0,T}^2. \tag{5.15}$$

The first column of Table 5.1 shows the exponent α of our artificial viscosity parameter h^α. The second column shows the ratios $Est_\alpha(\Omega)/Est_1(\Omega)$ of the estimated errors, and the last column the ratios of the true errors in the energy norm: The standard choice $\alpha = 1$ appears to be the

Table 5.1: Estimated and Actual Error Ratios for DCM.

α	Est_α/Est_1	Err_α/Err_1
1	1.00	1.00
3/2	1.81	1.02
2	4.07	1.91

best choice for globally smooth flow problems (without transition regions). We have repeated this experiment for more physically interesting flow problems (without a known exact solution – hence only finding the first column in the table). In these tests, the optimal artificial viscosity parameter again appeared to be $O(h^1)$. A similar trend was observed if the mini-element is used for the finite element discretization, see Table 5.2: We note that this result is a clear case when the $\alpha = 1$ result

Table 5.2: Estimated and Actual Error Ratios for DCM.

α	Est_α/Est_1	Err_α/Err_1
1	1.00	1.00
3/2	1.06	0.90
2	1.41	1.20

from optimizing the energy norm true and estimated error yields a different result from optimizing the celebrated 'eyeball' norm. For the latter case we obtained $\alpha = 2$, see test problem 5.2. We do not have a rigorous explanation of this discrepancy. For test problem 5.1, the estimated error was an accurate estimate of the true error for our choice of constants C_j. We observed, for example, with the mini-element: $Est_1^2(\Omega)/Err_1^2(\Omega) \approx 0.51/0.50 \approx 1.02$.

Test Problem 5.2. The Navier-Stokes equations with $f = 0$ and $g = 0$, adapted from Mohammadi and Pironneau [35]).

The domain Ω of this pipe cavity flow problem is shown in Figure 5.5. The Reynolds number is Reynolds number $1/Re = 1.75 \cdot 10^{-5}$ (see [13], [11] and [44]) The fluid flows in from the left (standard

paraboloid profile $\mathbf{u}_2(x,y) = 4y(1-y)$ along boundary $\{(x,y): x = 0, y \in [0,1]\}$) and out at the pipe's right end (with the same profile). The Dirichlet boundary conditions are homogeneous except for the pipe's in and out flow boundaries (the tests in [11] use Neumann boundary conditions on the outflow boundary of the pipe, the validity of either boundary conditions can be argued).

We expect at least three interesting physical structures to appear at higher Reynolds number: A large recirculating region in the cavity, a seperation line near the cavity-pipe juncture, and very small recirculating eddy where the flow leaves the cavity to re-enter the pipe. The last two structures are expected to carry most of the energy of the flow field. First, we determine which order of artificial diffusion α gives the sharpest resolution of transition regions and physical structures. We use the mini-element in order to test the resolution as a function of α. The fine uniform grid in figure 5.1 contains approximately 20,000 triangles. The flow fields are shown in figures 5.2 – 5.4. The velocity

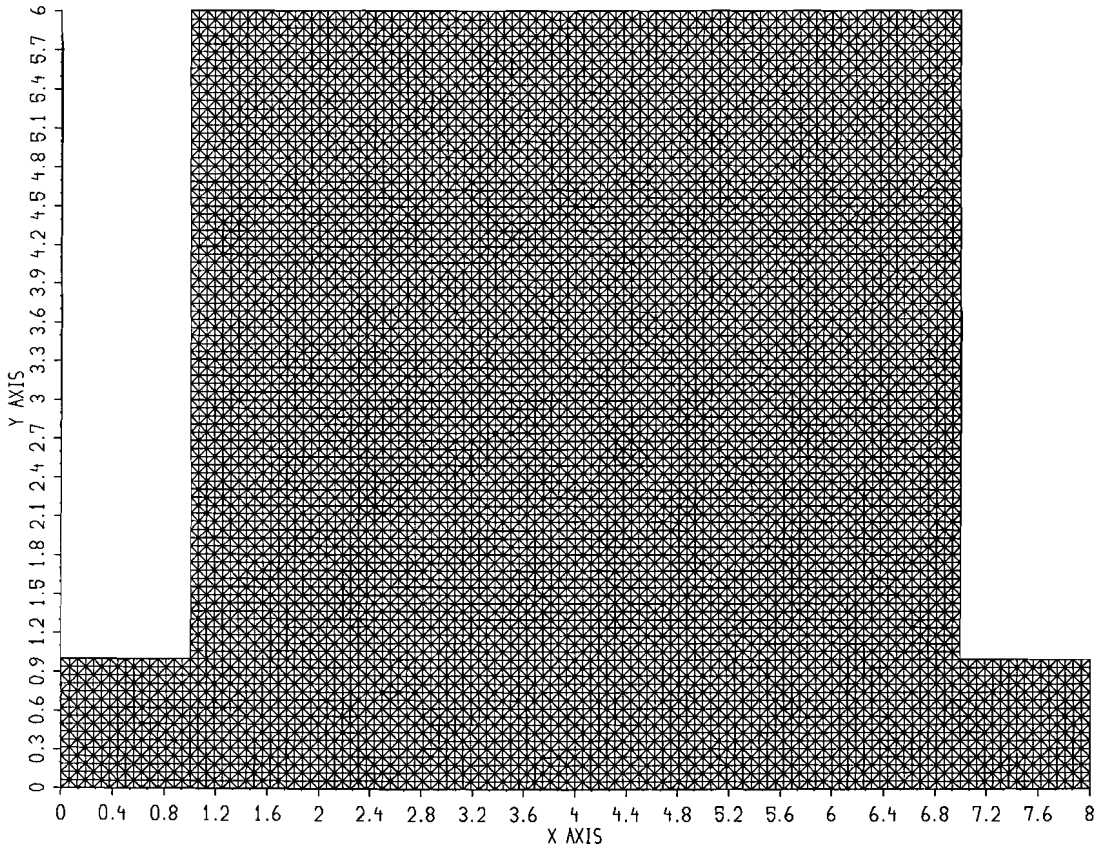

Figure 5.1: The uniform grid upon which the artificial viscosity parameter α is tested in figures 5.2 – 5.4.

vectors have been rescaled so that all arrows have the same length. Figure 5.2 indicates that a

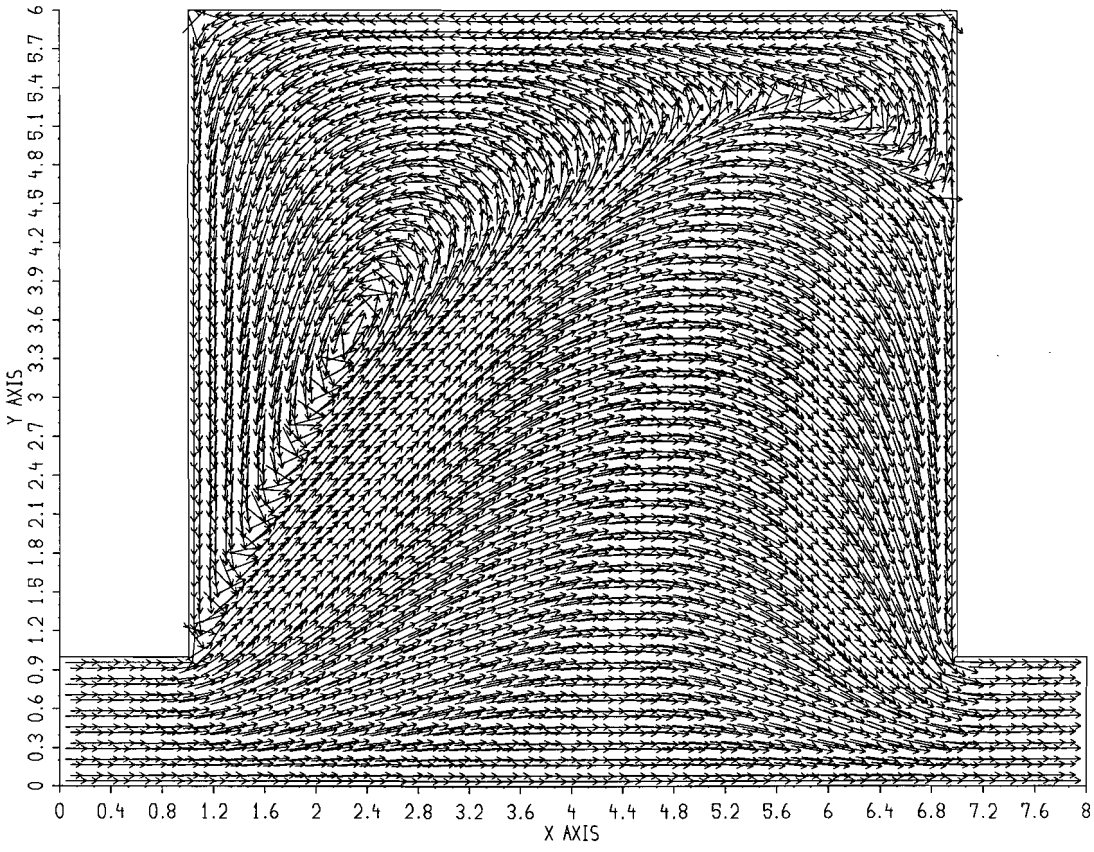

Figure 5.2: The $\alpha = 1$ flow field.

large amount of $O(h)$ viscosity is undesirable. The separation curve in the flow field computed with $O(h^2)$ artificial viscosity in figure 5.4 closely resembles the separation curve calculated in [35]. For our numerical test with adaptive refinement, we will therefore use $\alpha = 2$.

Next, Test problem 5.2 is solved with the use of adaptive refinement. Assume that the grid $\Pi^h(\Omega)$ contains $N(T)$ elements. For a given refinement threshold $C > 0$, a triangle T is refined if $Est_\alpha^2(T) > C/N(T)$, and a collection of descendant triangles T are taken out (de-refined) if they all satisfy $Est_\alpha^2(T) < C^2/2N(T)$. We set $C_1 = C_2 = C_3 = 1$ and use a refinement threshold $C = 4/10$.

The amount artificial viscosity is set to h^2 ($\alpha = 2$), and a Taylor-Hood finite element DCM discretization is used in combination with a r-Laplacian: $h^3|\nabla \mathbf{u}^{j-1}|$ subgrid scale model. The initial grid is shown in figure 5.5, and every second grid obtained by the adaptive refinement procedure is shown in figures 5.5 – 5.8. Figure 5.8 shows the finest grid, created by the adaptive refinement

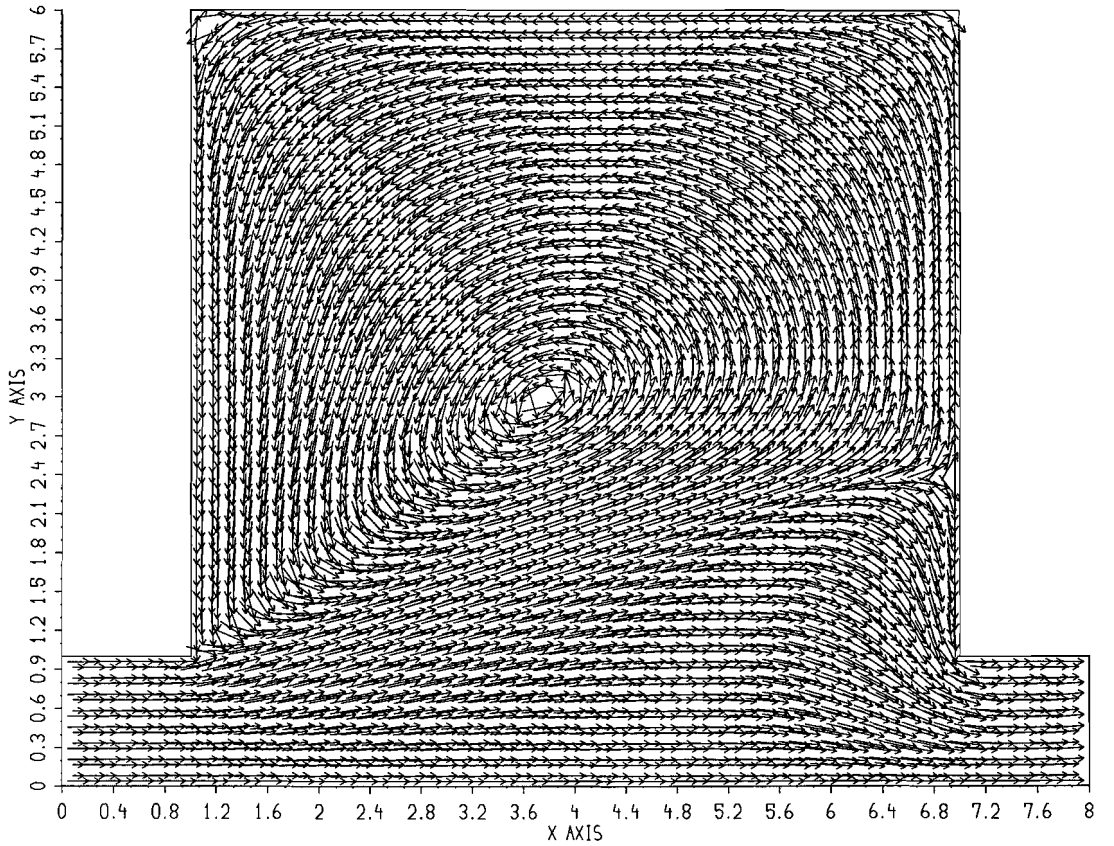

Figure 5.3: The $\alpha = 3/2$ flow field: A better approximation with $O(h^{3/2})$ artificial viscosity plus three corrections.

– based on the criterion described above. The amount of triangles is about 20,000. This is almost the same as in the case of the uniform refinement, but the adaptive refinement better resolves the regions of physical activity, because it is concentrated in the regions of expected physical activity. Along the boundaries of the inflow and outflow pipe the refinement take places, because the residual term $h_T^2 \|\mathbf{r}^{j+1}\|_{0,T}^2 + \|\nabla \cdot \mathbf{u}^{j+1} - g\|_{0,T}^2$ includes $\mathbf{u}\nabla\mathbf{u}$, which is large due to its not matching exactly the imposed outflow velocity. Further refinement is situated along a shear-layer/separation curve beginning at the reentrant corner $(1,1)$ and ends at a certain point along wall $\{(x,y): x = 7, y \in [1,7]\}$. This layer 'seperates' the fast flow through the pipe from the slower cavity flow. The velocity vector plot related to Figure 5.8 is shown in Figure 5.9. The plotting routine used sets all vectors to be of equal length, in order to make the circular cavity recirculating flow clearly visible. This round flow is much slower than the through flow and would hardly show up if vector were scaled proportional to their velocity. A magnification of the grid and related flow field is provided in figures 5.10 and 5.11.

These figures show the shear layer connects to the boundary of the cavity at a point which is

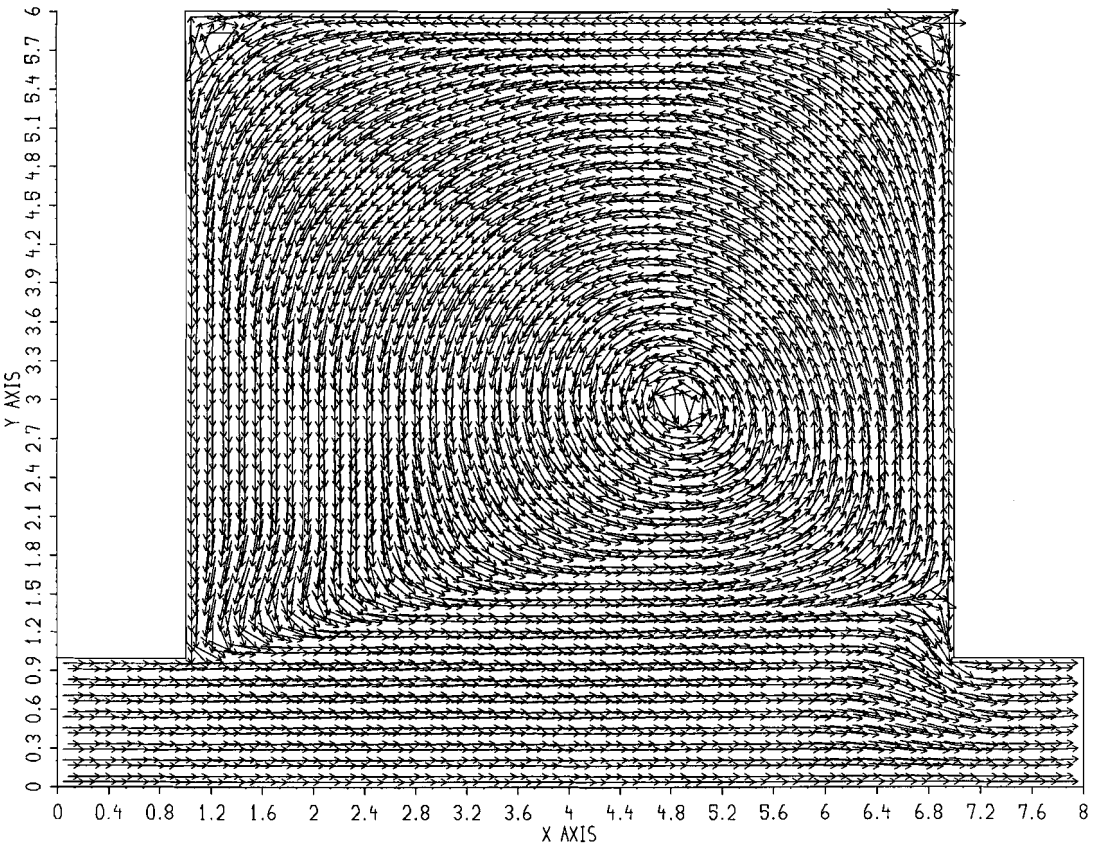

Figure 5.4: The $\alpha = 2$ flow field: $O(h^2)$ artificial viscosity plus three corrections yield the best resolution (uniform mesh).

situated lower than in the case of the uniform refinement. Furthermore, the adaptive refinement picks up a small vortex in the outflow pipe.

The amount of visible triangles E per grid G is shown in the third column of Table 5.3. The related number of degrees of freedom for velocity and pressure combined is provided in the second column. Finally, the maximum amount of non-linear iterations needed in order to solve all linearized systems is given in the last column.

The subgrid scale model used prevents non-physical solutions caused by overcorrecting in the DCM. For instance, in some computed approximate solutions to this problem with the mini-element without a subgrid scale model, we observed non-physical eddies in the left hand side which increased in number and decreased in size as the mesh was refined.

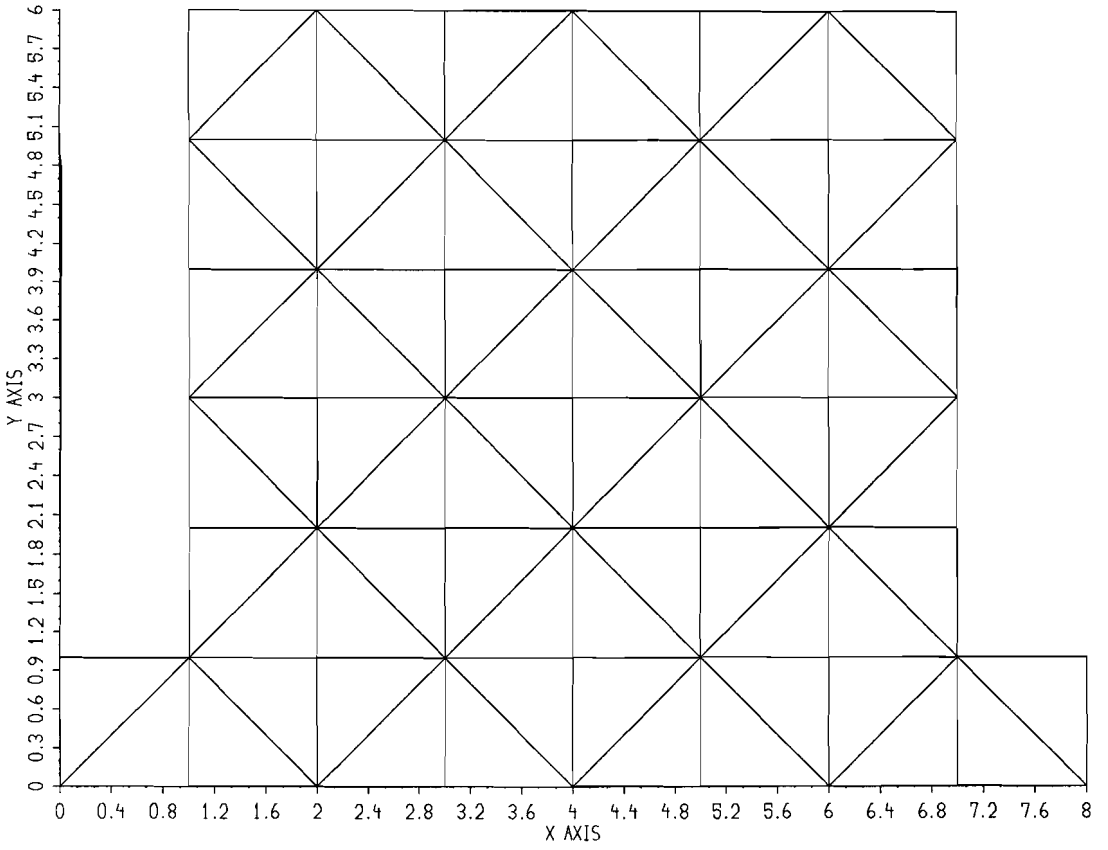

Figure 5.5: The initial grid for adaptive calculations.

6 Conclusions

Adaptive defect correction discretizations show great promise for approximating flows of incompressible viscous fluids at higher Reynolds numbers. The method is especially attractive since it is easy to introduce a subgridscale model (or turbulence model) into the calculation without significantly increasing the cost of resolving the nonlinearity in the system. In fact, we have seen that without simpel subgridscale models DCM can overcorrect and cause a limited number of non-physical small eddies to form. These are easily eliminated by the subgridscale model.

The use of a posteriori error estimators and self-adaptive algorithms is especially promising when a subgridscale model is used in the discretization. Specifically, when the error is estimated with respect to solutions of the unperturbed Navier-Stokes equations, a subgridscale model can be used with impunity to eliminate non-physical eddies.

We highly recommend the pipe driven cavity (test problem 5.2) as a challenging test problem, similar in spirit to the driven cavity but perhaps more physically reasonable.

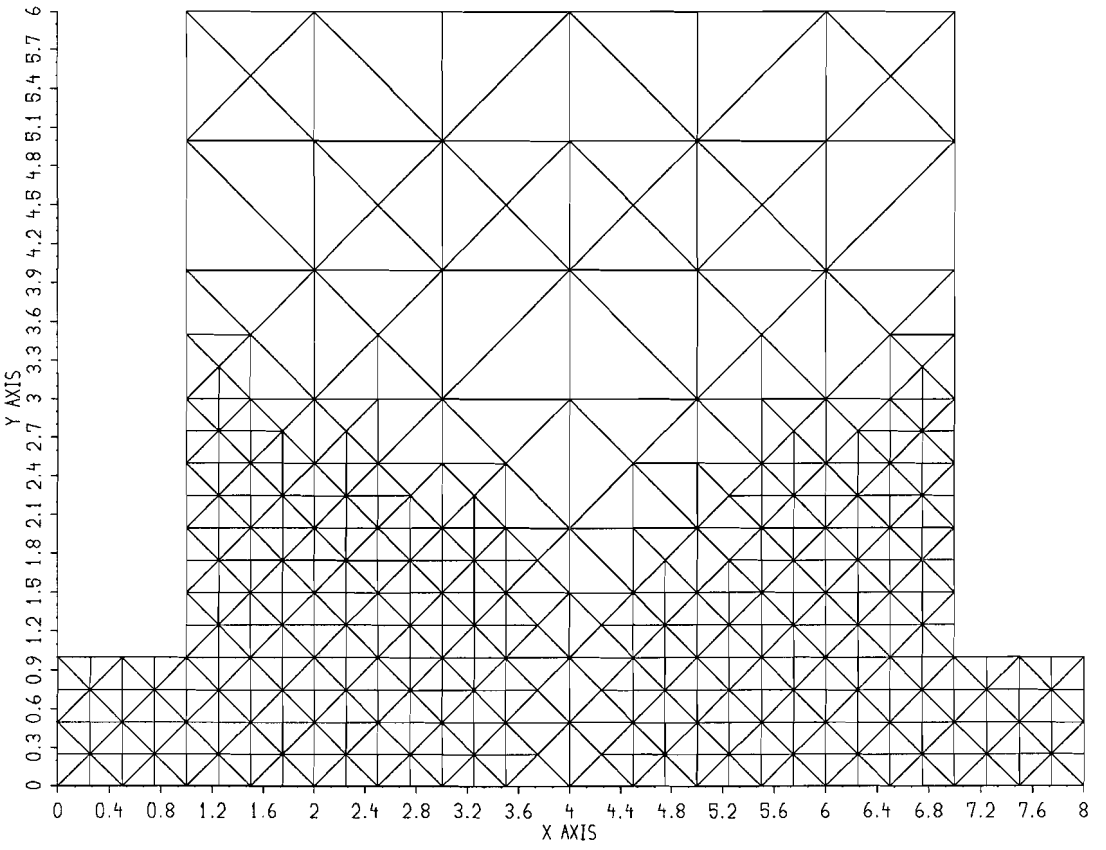

Figure 5.6: The second adaptively refined grid.

Based on the succes of the adaptive defect correction methods herein, two natural questions arise for further study: (1) Efficiency improvement of the method via for instance inexact solvers and the elimination of the artificial viscosity step from one grid to the next; (2) Analysis of the defect correction method applied at each time step in an evolutionary problem.

References

[1] D.N. Arnold, F. Brezzi and M. Fortin, "A stable finite element for the Stokes equations", *Calcolo* 21(1984), 337-344.

[2] O. Axelsson, "A restarted version of a generalized preconditioned conjugate gradient method", *Communications in Applied Numerical Methods* 4(1988) 521–530.

[3] O. Axelsson "Conjugate gradient type methods for unsymmetric and inconsistent systems of linear equations", *Linear Algebra Appl.* 29(1980) 1–16.

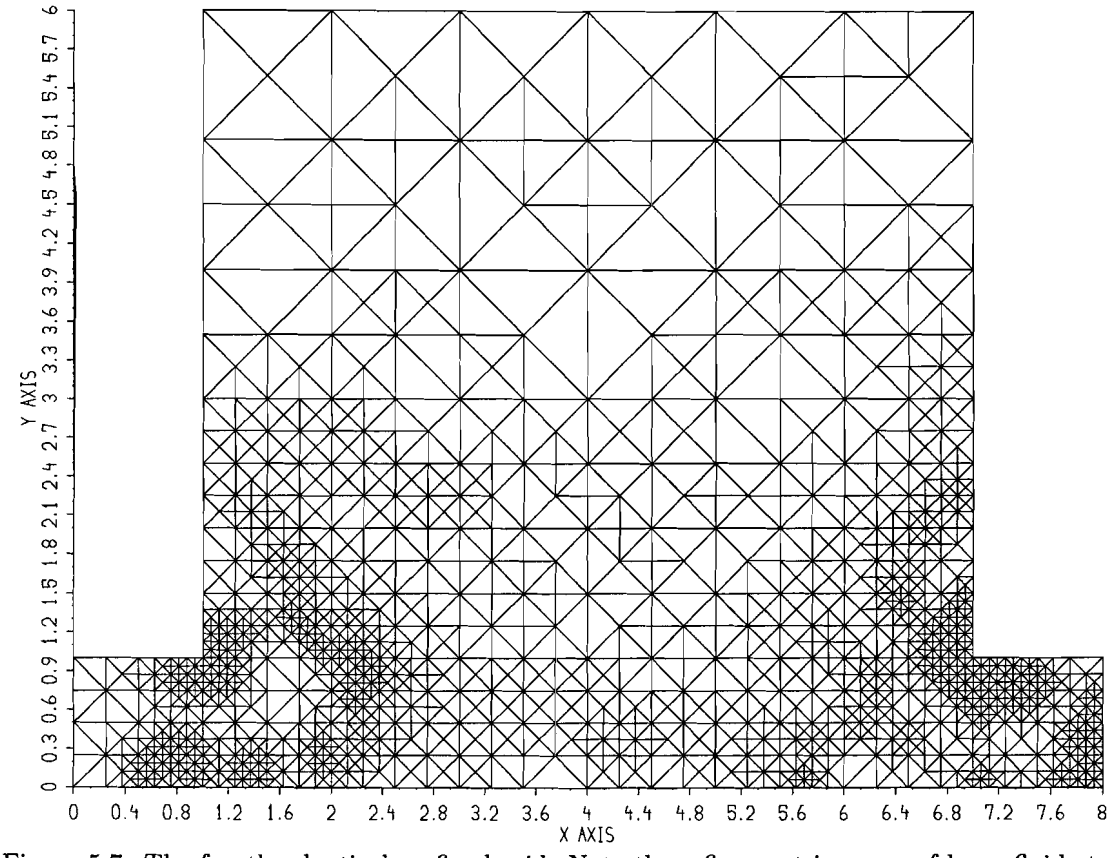

Figure 5.7: The fourth adaptively refined grid: Note the refinement in areas of large fluid stresses and at the approximate outflow boundary.

[4] Ainsworth, M. and Oden, J. T., "A unified approach to a posteriori error estimation using element residual methods", *Numer. Math.* 65(1993) 23-50.

[5] Axelsson, O. and Layton, W., "Defect correction methods for convection dominated, convection diffusion equations", *RAIRO J. Numer. Anal.* **24** (1990) 423-455.

[6] Axelsson, O. and Layton, W., "Iterative methods as discretization procedures", in *Preconditioned Conjugate Methods*, (eds: O. Axelsson and Y. Lu. Kolotilina), Springer LNM vol. 1457, Springer, Berlin, 1991.

[7] Babuska, I. and Rheinboldt, W. C., "Error estimates for adaptive finite element computations", *SIAM J. N. A.* 15(1978) 736-754.

[8] Babuska, I. and Miller, A., "A Posteriori error estimates and adapative techniques for the finite element method", U. of Maryland, Tech. Note BN-968, 1981.

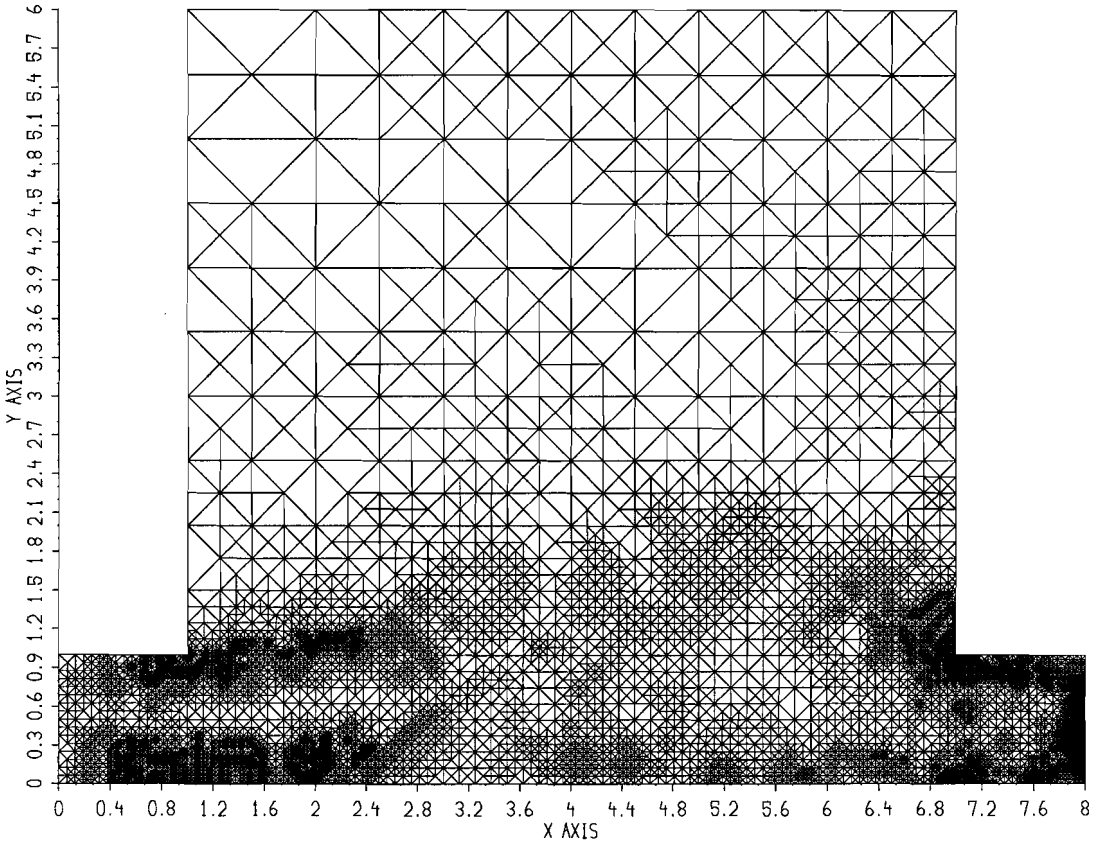

Figure 5.8: The sixth adaptively refined grid. Note the concentration of refinement in areas of physical activity.

[9] Bank, R. E. and Weiser, A., "Some a posteriori error estimators for elliptic partial differential equations", *Math. Comp.* 44(1985) 283-301.

[10] Bohmer, K., and Stetter, H. J., "Defect correction methods - Theory and Applications", Springer, Berlin, 1984.

[11] B. Cardot, B. Mohammadi and O. Pironneau' "A few tools for turbulence models in Navier-Stokes equations", **in** Incompressible Computational Fluid Dynamics (M.D. Gunzburger and R.A. Nicolaides, eds.), Cambridge University Press, Cambridge, 1993

[12] Clément, Ph., "Approximation by finite element functions using local regularization", *RAIRO Anal. Numér.* 2(1975) 77-84.

[13] G. Comte-Bellot, "Ecoulement turbulent entre deux paroix planes", Pub. Sci. et Tech. du Ministère del'air

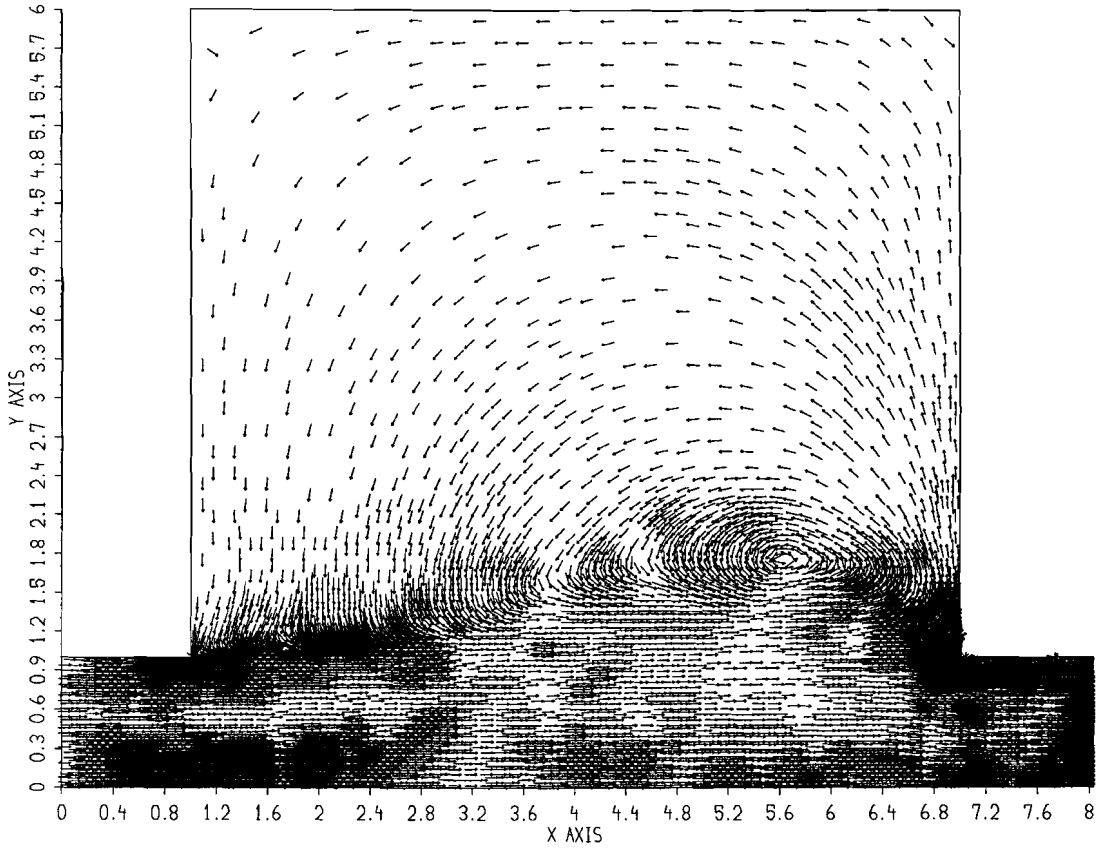

Figure 5.9: The flow field on the finest grid: All arrows are rescaled to be of equal size. A closeup view of the flow field in the right hand corner follows.

[14] R.S. Dembo, S.C. Eisenstat and T. Steihaug, "Inexact Newton methods", *SIAM J.N.A.* 19(1982), 400-408.

[15] Dunavant, "High degree efficient symmetric gauss quadrature rules for the triangle", *I.J.N.M.E.* 21(1985), 11291–11486.

[16] Eriksson, K. and Johnson, C., "Adaptive streamline diffusion finite element methods for stationary convection-diffusion problems", *Math. Comp.* **60** (1993) 167-188.

[17] Ervin, V. and Layton, W., "High resolution, minimal storage algorithms for convection dominated, convection diffusion equations", *Trans. Fourth Army Conf. on Appl. Math. and Computing* (1987) 1173-1201.

[18] Ervin, V. and Layton, W., "A study of defect correction, finite difference methods for convection diffusion equations", *SIAM J. N. A.* 26(1989) 169-179.

[19] Ervin, V., Layton, W. and Maubach, J., Report in Preparation, 1995.

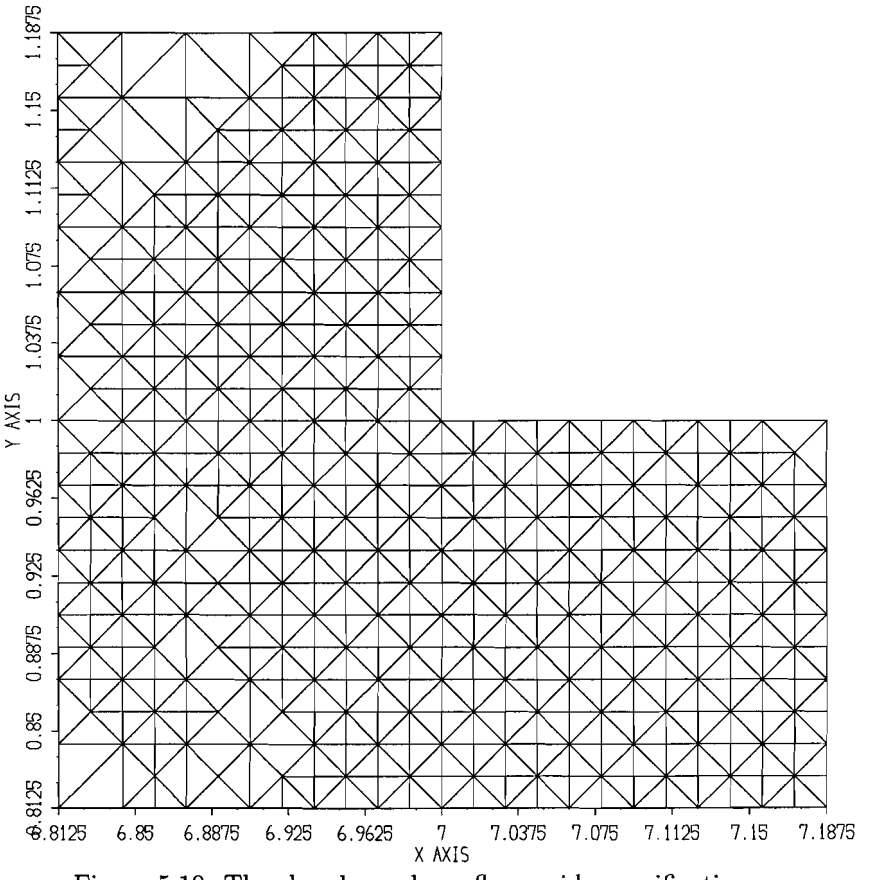

Figure 5.10: The shearlayer down flow, grid magnification.

[20] Girault, V., and Raviart, P.-A., "Finite element methods for Navier-Stokes equations. Theory and algorithms", Springer Verlag, Berlin, 1986.

[21] Gunzburger, M., "Finite element methods for viscous incompressible flows. A guide to theory, practice and algorithms", Academic Press, Boston, 1989.

[22] Hackbusch, W., "On multigrid iterations with defect correction", in *Multigrid Methods*, (eds: W. Hackbusch and V. Trottenberg), Springer LNM vol. 960, Springer, Berlin, 1982.

[23] Hackbusch, W., "Multigrid methods and applications", Springer, Berlin, 1985.

[24] Hemker, P., "Mixed defect correction iteration for the accurate solution of the convection difusion equation", in *Multigrid Methods*, (eds: W. Hackbusch and V. Trottenberg), Springer LNM vol. 960, Springer, Berlin, 1982.

[25] Hemker, P., "An accurate method without directional bias for the numerical solution of a 2-D elliptic singular perturbation problem", in *Thy. and Appls. of Sing. Perts.*, (eds: W. Eckhaus and E. M. de Jaeger), Springer LNM vol. 942, Springer, Berlin, 1982.

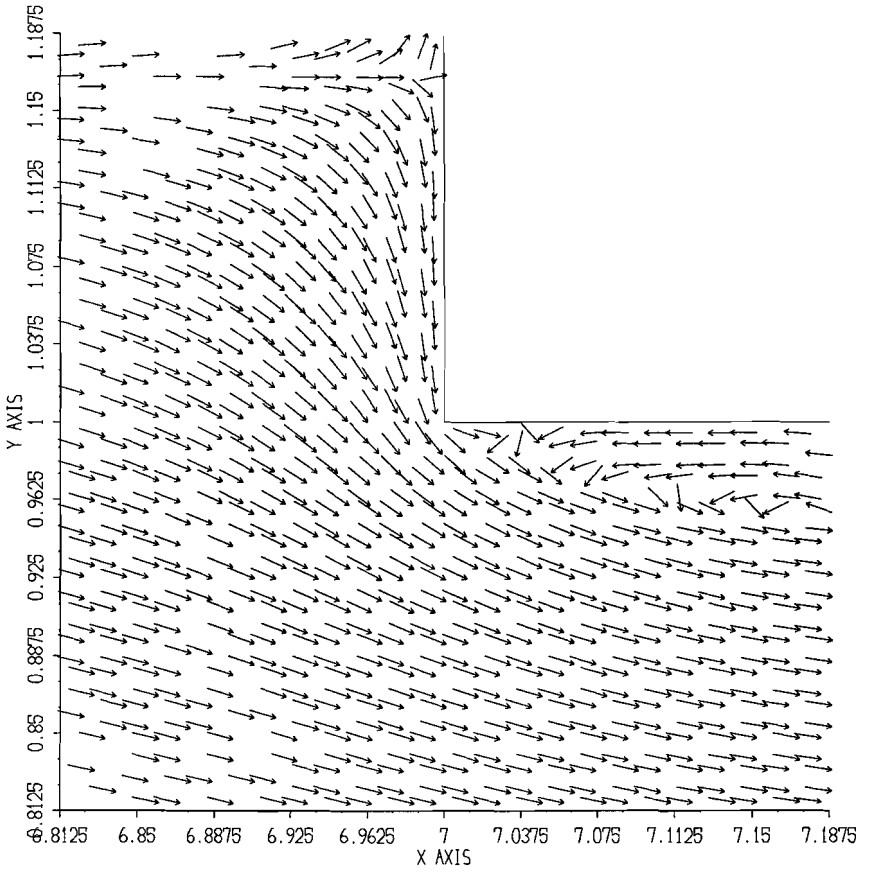

Figure 5.11: The shearlayer down flow, flow field magnification. Note: A recirculating eddy is captured in this adaptive calculation (not in our uniform mesh simulation, nor in the k-ϵ simulations).

[26] Hemker, P. and Koren, B., "Defect correction and nonlinear multigrid for the steady Euler equations", in *Advances in C. F. D.*, (eds: W. G. Habashi and M. M. Hafez), Cambridge Univ. Press, Cambridge, 1992.

[27] Hemker, P. and Koren, B., "Multigrid, defect correction and upwind schemes for the steady Navier-Stokes equations", in *Numer. Meth. for Fluid Dynamics III*, (eds: K. W. Morton and M. J. Baines), Clarendon Press, Oxford, 1988.

[28] Koren, B., "Multigrid and defect correction for the steady Navier-Stokes equations, Applications to Aerodynamics" C. W. I. Tract 74, Centrum voor Wiskunde en Informatica, Amsterdam, 1991.

[29] H. Kwon, W. Layton and J. Peterson, "Numerical solution of the stationary Navier-Stokes equations using a multi-level finite element method", Submitted, preprint available, Pittsburgh, U.S.A., 1996.

Table 5.3: Degrees of freedom and amount of Newton iterations ($\alpha = 2$).

#Grid	#Degrees of Freedom	#Triangles	#Newton It.
0	415	76	3
1	1311	264	3
2	2893	600	3
3	5885	1246	3
4	11315	2436	3
5	30601	6674	3
6	85524	18778	3

[30] Layton, W., "Solution algorithms for incompressible viscous flows at high Reynolds number", Vestnik Mosk. Gos. Univ., Series 15, No. 1(1996), 25-35.

[31] Layton, W., "A nonlinear subgridscale model for incompressible viscous flow problems", SIAM J. Sci. Comput. 17(1996), 347-357.

[32] J. Maubach, "Local bisection refinement for n-simplicial grids generated by reflections", *SIAM J. Sci. Comput.* 16(1995) 210-227.

[33] J. Maubach, "The amount of similarity classes created by local n-simplicial bisectionrefinement", submitted (preprint available), Pittsburgh, PA., USA, 1996.

[34] Rheinboldt, W. C. and Liu, J. L., "Á Posteriori error estimates for parameterized nonlinear equations", ICMA Report 90-151, 1990.

[35] B. Mohammadi and O. Pironneau, "Analysis of the k-ϵ Turbulence Model", Wiley, Chichester, 1994

[36] Y. Saad and M. H. Schultz, "GMRES: A generalized minimal residual algorithm for solving nonsymmetric linear systems", *SIAM J. Sci. Stat. Comput.* 7(1986), 856–869.

[37] P. Sonneveld, "CGS, a fast Lanczos-type solver for non-symmetric linear systems", *SIAM J. Sci. Stat. Comput.* 10(1989), 36–52.

[38] Stetter, H. J., "The defect correction principle and discretization methods", *Numer. Math.* 29(1978) 425-443.

[39] A. H. Stroud, "Approximate Calculation of Multiple Integrals", Prentice-Hall (Series in Automatic Computation), New York, 1971.

[40] C. Taylor and P. Hood, "A numerical solution of the Navier-Stokes equations using the finite element method", *Comput. & Fluids* 1(1973), 73-100.

[41] J. Todd Michael, "The Computation of Fixed Points and Applications, Lecture Notes in Economics and Mathematical Systems 124", Springer Verlag, Berlin, 1967.

[42] S. Vanka, "Block-implit multigrid calculation of two-dimensional recirculating flows", *Comp. Meth. Appl. Mech. Engrg.* 59(1986), 29-48.

[43] Verfürth, R., "A review of a posteriori error estimation and adaptive mesh refinement techniques", Seminar notes, Univ. Magdeburg, June 1993.

[44] P.L. Viollet, "On the modelling of turbulent heat and mass transfers in computations of buoyancy affected flows", Proc. Lat. Conf. Num. Meth. for Laminar and Turbulent Flows, Venezia

[45] O. Zienkiewicz, "The Finite Element Method in Engineering Science, 3^{rd} edition", Mc Graw-Hill, New York, 1977.